http://doi.org/10.29227/IM-2021-02-31 Received: 04 Jun 2021, Accepted: 09 Sep 2021, Published: 10 Nov 2021

Influence of Single-Phase Voltage Loss and Load Carrying Mode on Mine Drainage Pump Motor in Vietnam

DO Nhu Y[1], NGO Xuan Cuong[2,*]

[1] Hanoi University of Mining and Geology, 18 Vien street, Hanoi, Vietnam

[2] School of Engineering and Technology, Hue University, Hue, Vietnam

Corresponding author: ngoxuancuong@hueuni.edu.vn

Abstract. Mine drainage pump is the most important load in mining which requires high reliability when operating. Currently, the power supply of a mine drainage pump is connected to the same power line with many nonlinear loads, and is equipped with power electronic converters, which makes the power supply nonsinusoidal. During the working process of a mine drainage pump, the load-carrying factor often changes, and many types of failures occur, among which single-phase voltage loss is the most common problem. In the case of a nonsinusoidal power supply, if a single-phase voltage loss occurs in different load modes, it will greatly affect the working mode of the mine drainage pump leading to influences on the working efficiency, the life of the pump, and sometimes it is necessary to recalculate the protection parameters. This paper studies the influence of single-phase voltage loss and load carrying mode on the working mode of mine drainage pump motor in case the of nonsinusoidal power supply. Research results show that, in the case of nonsinusoidal power supplied with single-phase voltage loss, copper losses in the rotor and stator circuits increase with increases in voltage total harmonic distortion (THD) and load-carrying factor, 5th order reverse harmonic increases copper loss in asynchronous motor the most, and higher harmonic components have less effect on copper loss in the motor. At the same time, the speed ripple decreases with the increase of the motor load factor and decreases in the presence of the 5th order negative sequence harmonic, and increases significantly in the presence of the 7th order positive sequence harmonic. 5th order negative sequence harmonic increases, the torque ripple increases, while the 7th order positive sequence harmonic reduces the torque ripple in the case of single-phase voltage loss. The results of the paper will help improve the operational efficiency of the mine drainage pump in Vietnam's mines.

Keywords: Mine drainage pump, Single-phase voltage loss, Asynchronous motor, Harmonics

1. Introduction

The mine drainage pump is responsible for draining water during the mining process, ensuring timely drainage in mining even in adverse cases such as heavy rain, water breaks. Drainage pump is the most important load with the largest power consumption in mining [1]. Improving the performance of drainage pumps is of interest to many researchers. Drain pump performance needs to be checked periodically and it is always necessary to implement solutions to improve the energy efficiency of the pumping system [2, 3]. The characteristics of mining are wet and harsh environment, strong vibrations on working equipment due to drilling and blasting, transportation and unstable geology. This leads to many problems with the drainage pump motor in the mine, the most common being a single-phase voltage loss. In the case of a single-phase voltage loss, the motor will continue to operate but will also heat up very quickly and it is necessary to have solutions to improve operating efficiency as well as take measures to protect the motor when this operating mode occurs [4, 5, 6].

The progression to a single-phase voltage loss can take a long time from uncertain electrical contacts, loose connections, and gradually progressing to the single-phase voltage loss. The above progression results in an electrical imbalance. Under an unbalanced voltage, the amplitude of the current deviation can be many times larger and generate torque impulse. These problems lead to reduced performance of the motor, overheating, damage [7, 8]. The article [9] studied the impact of unbalanced voltage supply on the performance of a 3-phase induction motor. The results showed that the voltage imbalance leads to reduced motor efficiency and reduces power factor. Unbalanced voltages in a voltage source can lead to problems such as excessive losses, overvoltage, mechanical oscillations, and interference with electrical equipment [10]. Unbalanced voltage has a marked effect on the losses in the induction motor, which greatly affects the winding temperature rise and the slip coefficient. Several literary studies have also shown that the power factor of the asynchronous motor is inversely proportional to the positive sequence, while the efficiency is directly proportional to the positive sequence [11, 12, 13, 14].

The effect of voltage asymmetry on the operation of the asynchronous motor has been analyzed in [15] [16]. Gnacinski et al. [16] revealed that the voltage imbalance causes coil heating much faster than the effects of other power quality standards [17]. The characteristics of the 6kV power network supplying power to mine water pump systems in Vietnam have along outgoing lines, use high-powered equipment, multiple branches, and increasing use of power electronics on the grid, this reduces the quality of the voltage supplied to the drain pump motors and affects the performance characteristics of the motors [18, 19]. The voltage quality of the power supply to a mine water pump motor when connected through the converter is often influenced by harmonic components [20, 21].

In [8], Bhattarai identified power quality problems and their impact on power systems and loads. It was also suggested in that paper that harmonics have a significant influence on the current capacity of various electrical components, such as cables, transformers and power transmission lines and electric motors. The supply of pulse-width modulation inverter causes an additional loss, which is manifested as a temperature rise in the asynchronous motor. The temperature rise due to additional losses is significant compared with machines operated from sinusoidal sources [22]. In [23], the authors have shown the existence of harmonics in power systems generated by non-linear loads, such as power electronic devices, electric arc furnaces, and the presence of this harmonic greatly affects the performance of the asynchronous motor. When powered with a high harmonic voltage, an asynchronous motor will experience increased vibration [24].

The selection of mine drainage pump capacity is based on the rated working capacity of the mine drainage design. However, the drainage pump is operated in different modes depending on the actual requirements of the mine drainage, the quality of mine wastewater changes causing the pump load to change. At the same time, the use of drainage pumps in the whole mining cycle is also the difference in pump capacity compared to the design capacity, which affects the working mode of the mine drainage pump [1]. In [25], the authors have shown the effect of unbalance due to frequency deviation according to the load-carrying factor of the motor on the loss, temperature rise, torque, efficiency of the motor as well as vibration and reliability when the motor is working. Different case studies were presented with different load conditions to study the performance of electromechanical systems widely used in the mining industry [26]. The results indicated that severe torque will be generated on the motor shaft during starting. This severe torque can lead to an effect on the life of the crankshaft if appropriate countermeasures are not taken.

From the above analyses, it is necessary to study the effect of single-phase voltage losses and the load-carrying mode considering the influence of the power supply on the mine drainage pump motor. The research results are important data for users to have suitable operating solutions to improve the operating efficiency and life of the mine drainage pump motor in different operating modes.

2. Materials and Methods

2.1 Model of asynchronous motor

Mine drainage pumps in Vietnam are usually driven by asynchronous motors (AM). The AM electrical part is represented by a quaternary state space model and the mechanical part by a quadratic system [19, 27]. All stator and rotor quantities are in an arbitrary biaxial reference frame (dq frame) in Fig. 1. The physical model is considered to be linear and the inductance is assumed to be constant. Therefore, the saturation of the magnetic circuit is not considered here.

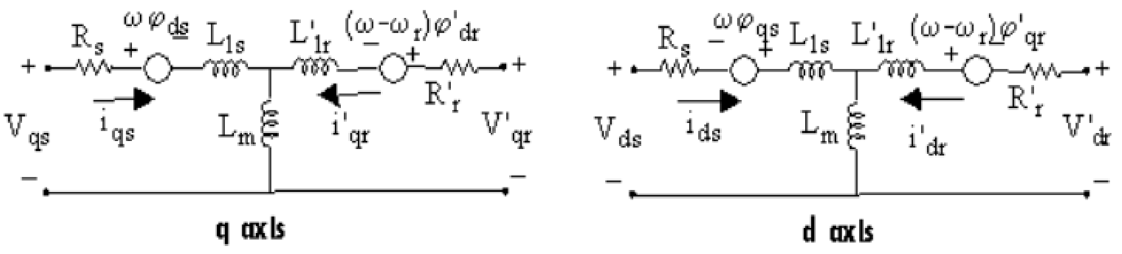

Fig. 1. The AM Model on the qd frame.

Synchronous speed is determined by:

$$N_s = \frac{60.\mathrm{f}}{\mathrm{p}} \tag{1}$$

where f - frequency, p - number of double poles. Rated torque is determined by:

$$T_n = \frac{30.\mathrm{P_n}}{\pi.\mathrm{N_n}} \tag{2}$$

where P_n - power, N_n – speed.

When the power source has harmonics, power factor (PF) is calculated according to the following relationship:

$$PF = \frac{\mathrm{P_{in}}}{\sqrt{\mathrm{P_{in}^2} + \mathrm{Q_{in}^2}}} \tag{3}$$

where P_{in} - the active input power in W, Q_{in} – the reactive input power in Var. The mechanical power is calculated according to the following formula:

$$P_{-M} = \mathrm{T_e}.\omega_\mathrm{m} \tag{4}$$

where T_e - electromagnetic torque in Nm, ω_m - angular velocity of the rotor in rad/s. The mechanical loss is determined according to the following formula

$$P_{\_loss\_m} = F.\omega_\mathrm{m}^2 \tag{5}$$

where F represents the friction factor in N.m.s. The losses in the motor mainly occur in the rotor, stator circuit and ferromagnetic losses. In this model of asynchronous motor, ferromagnetic losses are ignored. The copper loss on the rotor is determined by:

$$P_{Cu2} = R_r'\left(I_{ra}^2 + I_{rb}^2 + I_{rc}^2\right) \tag{6}$$

where I_{ra}, I_{rb}, I_{rc} - RMS value of rotor current in phase a, b, c, R'_r - rotor resistance. The copper loss on the stator is determined by:

$$P_{Cu1} = R_s\left(I_{sa}^2 + I_{sb}^2 + I_{sc}^2\right) \tag{7}$$

where I_{sa}, I_{sb}, I_{sc} - RMS value of stator current in phase a, b, c, R_s - stator resistance.

Finally, we determine the AM efficiency using the direct method as follows:

$$\eta = \frac{P_{-M} - P_{-loss-m}}{P_{in}}100 \tag{8}$$

where P_{in} - the active input power in W, P_{-M} - the total mechanical power of motor in W, $P_{-loss-m}$ - the mechanical losses (friction and windage losses), in W.

2.2 Model to evaluate the single-phase voltage loss

Assuming that the asynchronous motor is working, a single-phase voltage loss occurs with a replacement diagram shown in Fig. 2 [4].

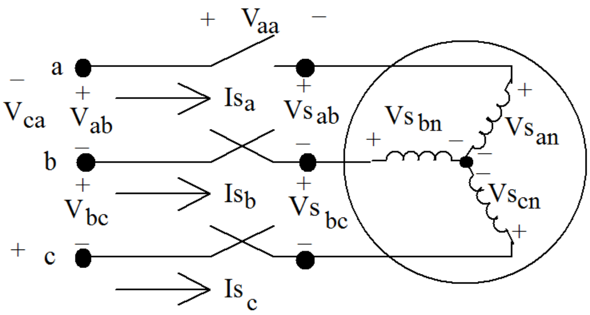

Fig. 2. Loss of phase a of asynchronous motor [4].

http://doi.org/10.29227/IM-2021-02-31 Received: 04 Jun 2021, Accepted: 09 Sep 2021, Published: 10 Nov 2021

where V_{ab}, V_{bc}, V_{ca}- line-to-line voltage of the system, V_{sab}, V_{sbc}, V_{sca} - working line voltage at motor terminal, $V_{s.an}$, $V_{s.bn}$, $V_{s.cn}$ - stator line-to-neutral voltage, I_{sa}, I_{sb}, I_{sc} -line current.

When a motor has a single-phase voltage loss, the voltage and current on the motor can be decomposed into the components of positive order (index 1), negative order (index 2) and zero order (index 0). The replacement diagram for single-phase voltage loss is shown in Figure 3.

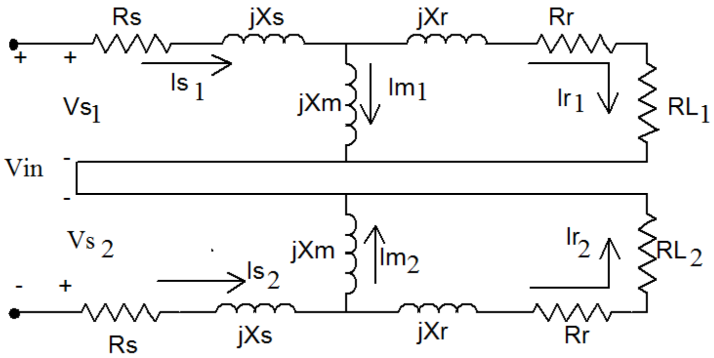

Fig. 3. Sequence Network Connection [4].

where V_{in}- input voltage, R_s, X_s – resistance and reactance of stator circuit, R_r, X_r – resistance and reactance of rotor circuit, X_m- magnetizing reactance, RL – load impedance.

The input voltage is given by:

$$V_{in} = V_{s1} - V_{s2} \tag{9}$$

The input voltage according to the case of phase loss can be calculated as:

$$\begin{gathered} V_{s1} = \frac{1}{3}(V_{s.an} + aV_{s.bn} + a^2V_{s.cn}); \\ V_{s2} = \frac{1}{3}(V_{s.an} + a^2V_{s.bn} + aV_{s.cn}) \\ V_{in} = V_{s1} - V_{s2} = j\frac{\sqrt{3}}{3}(V_{s.bn} - V_{s.cn}) = j\frac{V_{s.bc}}{\sqrt{3}} \end{gathered} \tag{10}$$

Then the negative sequence slip is given by:

$$s_2 = 2 - s_1 \tag{11}$$

The load resistances of the two networks are:

$$\begin{gathered} RL_1 = \frac{1 - s_1}{s_1}\mathrm{R_r} \\ RL_2 = \frac{1 - s_2}{s_2}\mathrm{R_r} = \frac{1 + s_1}{2 - s_1}\mathrm{R_r} \end{gathered} \tag{12}$$

The general equation for the input equivalent impedance at the terminals of the networks is given by:

$$Z_{eqi} = \mathrm{Z_{si}} + \frac{\mathrm{Z_r} - RL_i}{\mathrm{j}X_m + \mathrm{Z_r} + RL_i} \tag{13}$$

where i = 1 for the positive sequence and i = 2 for the negative sequence.

The stator sequence currents are:

$$\begin{gathered} I_{s1} = \frac{\mathrm{V_{in}}}{Z_{eq1} + Z_{eq2}} \\ I_{s2} = -I_{s1} \\ I_{s0} = 0 \end{gathered} \tag{14}$$

Because the motor is connected to a three-wire delta line, the zero sequence stator current must be zero. The stator input line currents are computed by:

$$\begin{bmatrix} I_{sa} \\ I_{sb} \\ I_{sc} \end{bmatrix} = \begin{bmatrix} 1 & 1 & 1 \\ 1 & \mathrm{a} & \mathrm{a}^2 \\ 1 & \mathrm{a}^2 & \mathrm{a} \end{bmatrix} \begin{bmatrix} I_{s0} \\ I_{s1} \\ I_{s2} \end{bmatrix} \tag{15}$$

The sequence rotor currents are determined by:

$$I_{ri} = \mathrm{I_{si}} - \frac{\mathrm{j}X_m}{\mathrm{j}X_m + \mathrm{Z_r} + RL_i} \tag{16}$$

- Motor Terminal Voltages:

$$\begin{gathered} V_{s0} = 0 \\ V_{si} = Z_{eqi} - I_{si} \end{gathered} \tag{17}$$

The sequence line-to-neutral stator voltages are:

$$\begin{bmatrix} V_{s.an} \\ V_{s.bn} \\ V_{s.cn} \end{bmatrix} = \begin{bmatrix} 1 & 1 & 1 \\ 1 & \mathrm{a} & \mathrm{a}^2 \\ 1 & \mathrm{a}^2 & \mathrm{a} \end{bmatrix} \begin{bmatrix} V_{s0} \\ V_{s1} \\ V_{s2} \end{bmatrix} \tag{18}$$

The line-to-line stator voltages are:

$$\begin{bmatrix} V_{s.ab} \\ V_{s.bc} \\ V_{s.ca} \end{bmatrix} = \begin{bmatrix} 1 & -1 & 0 \\ 0 & 1 & -1 \\ -1 & 0 & 1 \end{bmatrix} \begin{bmatrix} V_{s.an} \\ V_{s.bn} \\ V_{s.cn} \end{bmatrix} \tag{19}$$

It needs to be pointed out that the stator line-to-line voltages will not be the same as the secondary line-to-line voltages. Because this voltage will appear across the switch (fuse), it is given by:

$$V_{aa} = V_{ab} - V_{s.ab} \tag{20}$$

- Converted Power

The total converted sequence powers are given by:

$$P_{convi} = 3.I_{ri}^2.RL_i \tag{21}$$

We recall that the negative sequence load resistance is a negative number so that the converted negative sequence power will be negative, which adds to the effective rotor power loss. The total converted power is:

$$P_{convi} = P_{conv1} + P_{conv2} \tag{22}$$

- Stator and Rotor Power Losses

The total stator and rotor power losses are:

$$\begin{gathered} P_{loss.rotor} = 3(I_{r1}^2 + I_{r2}^2)R_r \\ P_{loss.stator} = 3(I_{s1}^2 + I_{s2}^2)R_s \end{gathered} \tag{23}$$

2.3 Model of harmonics

Drain pump motors in Vietnam's mines are usually powered by power converters (i.e., soft starters or inverters) with the actual form shown in Figure 4. Power converters often cause a large number of harmonics on the grid, so it is necessary to build a harmonic effect on the motor.

The equation for the motor supply voltage can be written as:

$$\begin{gathered} v_a = V_m sin\omega t \\ v_b = V_m sin\left(\omega t + \frac{2\pi}{3}\right) \\ v_c = V_m sin\left(\omega t - \frac{2\pi}{3}\right) \end{gathered} \tag{24}$$

A non-sine waveform can be constructed by adding two or more sine waves. The synthesis of a particular non-sine waveform is a problem of combining signals of appropriate frequency, amplitude, and phase. Using the "Thee Phase Programmable Voltage Source" block in Simulink can generate non-sine waveforms to power an asynchronous motor.

a) b)

Fig. 4. Power supply of a mine water pump motor in Vietnam: a mine drainage pump (left) and a conversion device (right).

Harmonic is a sinusoidal voltage whose frequency is an integer multiple of the fundamental power system frequency. Harmonics have the positive order ($k_p = 3n + 1$), the negative order ($k_n = 3n + 2$) and the zero order ($k_z = 3n$). In an asynchronous motor, when the motor windings are connected in a three-wire Y configuration with an isolated neutral, zero-sequence current harmonics is null. The total harmonic distortion (THD) in the current can be calculated by:

$$THD = \frac{\sqrt{\sum_{n=2}^{\infty} I_n^2}}{I_1} = \frac{\sqrt{I_1^2 + I_2^2 + I_3^2 + I_4^2 + \cdots}}{I_1} \quad (25)$$

Harmonics will affect the motor's losses according to Eq. (6) and Eq. (7), leading to a decrease in motor efficiency.

2.4 Modeling and simulation of research models

The main mine drainage pump motor parameter in this study is the FD450-60x4 motor type, whose nominal data and other characteristic dimensions are indicated in Table 1. This is a 3-phase squirrel cage rotor asynchronous motor, class F insulation, connected in the shape of Y. The model of mine drainage pump is show on Figure 5. We use a 3-phase asynchronous motor model in the Matlab-simulink library, version R2014a. The simulation parameters of the motor are calculated based on the parameters shown in Table 1.

Tab. 1. Main pump specifications FD450-60x4.

Parameter	Value	Parameter	Value
Flow (m^3/h)	450	Rated power, Pn (kW)	630
Push height (m)	262	Rated voltage, U (kV)	6
Pump efficiency (%)	80	RPM, Nn (rpm)	1493
NPSH (m)	5	Efficiency, η (%)	96.4
Diameter of straws (mm)	450	PF (%)	87
Diameter of push tube (mm)	350	Starting torque multiples	0.8
Total pump weight (kg)	7520	Starting current multiple	6.5

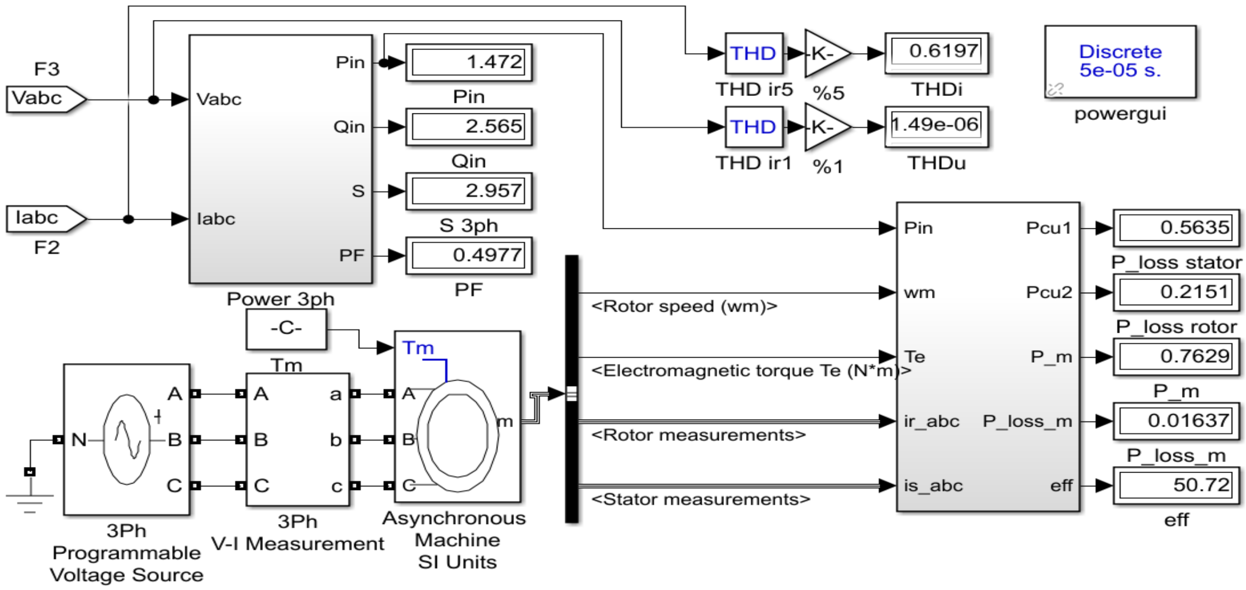

Fig. 5. Simulation model of the mine drainage pump motor.

Investigate motor working in the normal mode with three-phase power supply, we use sinusoidal power supply and motor's load-carrying factor K=100%. The results tested on the model are shown in Table 2 and in Figure 6.

Tab. 2. Parameters of the motor with sinusoidal voltage source.

Motor Load, %	Parameter							
	THD, %	Pcu_1, pu	Pcu_2, pu	N, rpm	Te, Nm	P_loss_m, pu	PF	η, %
75	0	0.0105	0.0027	1495	3089	0.0166	0.81	96.18
100	0	0.0160	0.0049	1493	4097	0.0165	0.87	96.40
125	0	0.0232	0.0076	1491	5104	0.0165	0.90	96.36

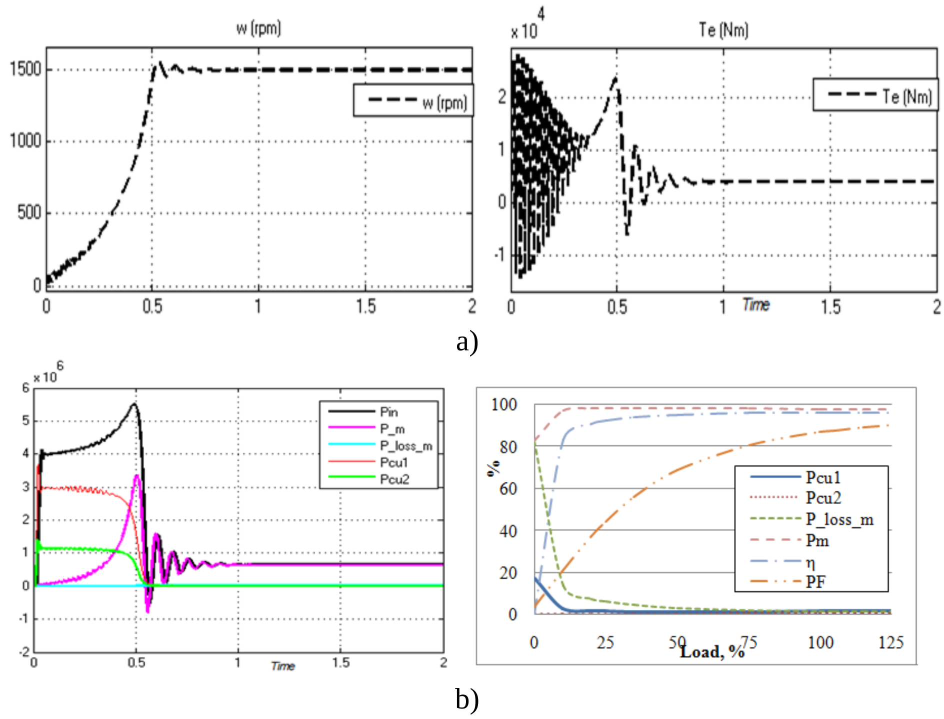

Fig. 6. Characteristics of the drainage pump motor when working in a normal mode with K=100%: a) Motor speed and torque, b) Loss components and motor efficiency.

http://doi.org/10.29227/IM-2021-02-31 Received: 04 Jun 2021, Accepted: 09 Sep 2021, Published: 10 Nov 2021

The results in Tables 2 and Figure 6 are similar to the rated parameters of the motor in Table 1. Thus, the model is built reliably.

3. Results and discussions

Using the simulation model built in Figure 5, the working mode of the mine drainage pump motor in different cases is tested. The proposed case study is a power supply containing harmonic components and single-phase voltage loss at 1.5s, the motor operates with a load factor of 75%, 100%, and 125%, respectively. THD of power supply is considered with values of 5%, 10%, 15%. Copper loss, ripple of torque and speed analyzed in source cases containing 5^{th}, 7^{th}, 11^{th} and 13^{th} harmonic components (corresponding to symbols are H5&LP, H7&LP, H11&LP, H13&LP). The obtained results are presented in Table 3.

Figure 7 shows the transient characteristics of the motor, torque and motor losses in the case of single-phase voltage loss at 1.5s with 100% load and 5th harmonic with THD=5%. From the results shown in Figure 7, when a single-phase voltage loss is accompanied by a harmonized power supply, the speed and torque of the asynchronous motor strongly fluctuate. This causes vibrations when working and an increase in the loss of the motor, leading to a reduction in the efficiency of the motor compared to the normal working mode.

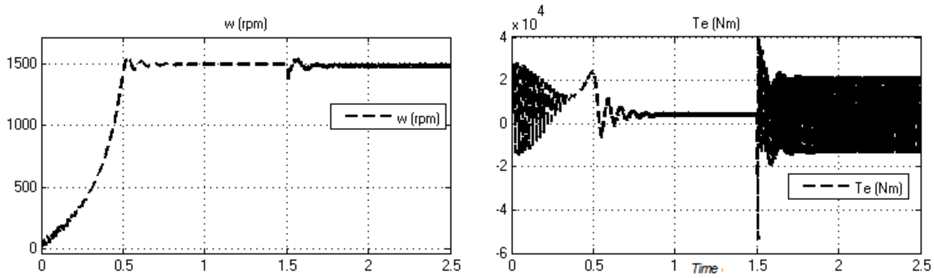

a)

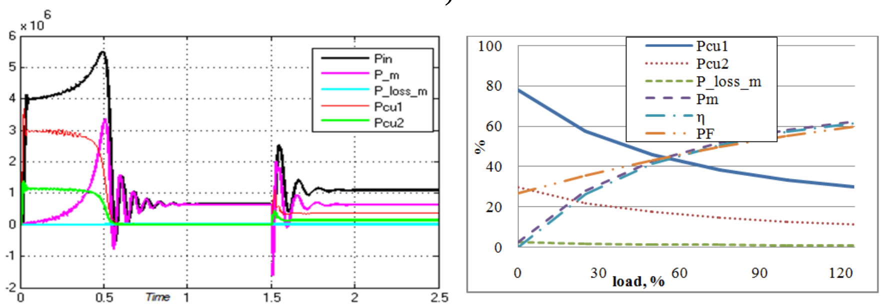

b)

Fig. 7. Characteristics of the drainage pump motor with K=100% in the case of single-phase voltage loss at 1.5s: a) Motor speed (w) and torque (Te), b) Loss components and motor efficiency.

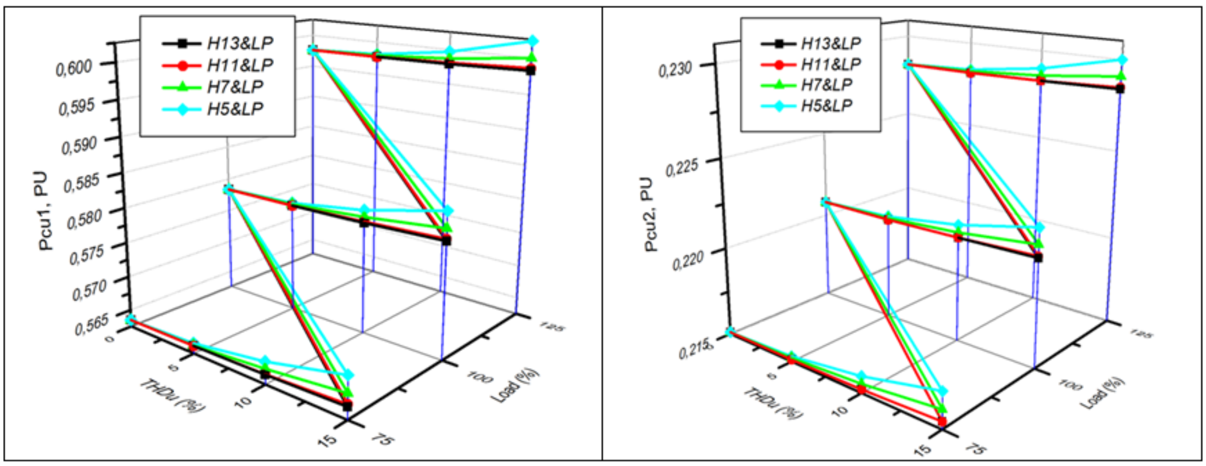

Fig. 8. Copper losses of the motor: Copper loss on stator (P_{Cu1}) and copper loss on rotor (P_{Cu2}).

Tab. 3. Motor performance parameters in the case of a single-phase voltage loss considering the load carrying factor and the effect of harmonics.

Load (%)	Harmonic	THDu, %	P_{cu1}, W pu	P_{cu2}, W pu	Ripple N, %	Torque ripple, %	P_{loss}, W pu
75	phase loss	0	0.5635	0.2151	1.575	1134	0.7786
	5th order harmonic (H5&LP)	5	0.5640	0.2153	1.561	1163	0.7793
		10	0.5656	0.2159	1.548	1194	0.7815
		15	0.5682	0.2169	1.536	1226	0.7851
	7th order harmonic (H7&LP)	5	0.5637	0.2152	1.586	1112	0.7789
		10	0.5646	0.2155	1.596	1091	0.7801
		15	0.5659	0.2160	1.607	1073	0.7819
	11thorder harmonic (H11&LP)	5	0.5636	0.2151	1.577	1120	0.7787
		10	0.5639	0.2152	1.578	1112.4	0.7791
		15	0.5645	0.2154	1.58	1112.8	0.7799
	13th order harmonic (H13&LP)	5	0.5636	0.2151	1.573	1146	0.7787
		10	0.5638	0.2152	1.572	1158	0.779
		15	0.5642	0.2154	1.571	1171	0.7796
100	phase loss	0	0.5783	0.2208	1.561	845	0.7991
	5th order harmonic (H5&LP)	5	0.5788	0.221	1.547	867.6	0.7998
		10	0.5804	0.2216	1.533	891	0.802
		15	0.583	0.2226	1.52	915	0.8056
	7th order harmonic (H7&LP)	5	0.5786	0.2209	1.572	827.6	0.7995
		10	0.5794	0.2212	1.583	810	0.8006
		15	0.5807	0.2217	1.594	795	0.8024
	11th order harmonic (H11&LP)	5	0.5784	0.2208	1.563	836	0.7992
		10	0.5788	0.2209	1.565	832	0.7997
		15	0.5793	0.2211	1.567	833.9	0.8004
	13th order harmonic (H13&LP)	5	0.5784	0.2208	1.559	853	0.7992
		10	0.5786	0.2209	1.557	861	0.7995
		15	0.579	0.221	1.555	871	0.8
125	phase loss	0	0.5976	0.2282	1.544	669.13	0.8258
	5th order harmonic (H5&LP)	5	0.5981	0.2284	1.53	687.46	0.8265
		10	0.5997	0.2290	1.516	706.35	0.8287
		15	0.6023	0.230	1.503	725.73	0.8323
	7th order harmonic (H7&LP)	5	0.5979	0.2283	1.556	654.72	0.8262
		10	0.5987	0.2286	1.567	640.52	0.8273
		15	0.6	0.2291	1.579	626.83	0.8291
	11th order harmonic (H11&LP)	5	0.5977	0.2282	1.547	663.18	0.8259
		10	0.5981	0.2283	1.549	661.59	0.8264
		15	0.5986	0.2285	1.552	664.17	0.8271
	13th order harmonic (H13&LP)	5	0.5977	0.2282	1.542	674.44	0.8259
		10	0.5979	0.2283	1.54	680.84	0.8262
		15	0.5983	0.2284	1.537	687.95	0.8267

From the results in Table 3, a graph depending on the working parameters of the motor is built. Figure 8 shows that copper losses in the rotor and stator circuits increase as the load-carrying factor and the voltage THD increase. When the motor loses single-phase voltage, the losses in the motor increase, and are highest in the case of a power source containing 5th harmonics. The increase in the THD harmonic index makes the motor loss increase. Therefore, it is necessary to limit the 5th harmonic component and reduce the harmonic amplitude in the power supply network to reduce the losses in the motor.

When the mine drainage pump motor with 75% load factor is working under a power supply containing 5th harmonics with THD={5%, 10%, 15%}, the stator copper loss increases by {1.05, 1.20, 1.45} times and the rotor copper loss increases by {1.07, 1.29, 1.66} times respectively compared with the symmetric sine power supply case. When the mine drainage pump motor with 100% load factor is working under a power supply containing 5th harmonics with THD={5%, 10%, 15%}, the stator copper loss increases by {1.03, 1.13, 1.29} times and the rotor copper loss increases by {1.04, 1.16, 1.37} times respectively compared with the symmetric sine power supply case.

When the mine drainage pump motor with 125% load factor is working under a power supply containing 5th harmonics with THD={5%, 10%, 15%}, the stator copper loss increases by {1.02, 1.09, 1.20} times and the rotor copper loss increases by {1.03, 1.11, 1.24} times respectively compared with the symmetric sine power supply case. When the mine drainage pump motor is overloaded with a load carrying factor of 125%, if a single-phase voltage loss occurs, the total copper loss in the motor will increase to 3.3% compared to the total copper loss when the single-phase voltage loss occurs at rated load K=100% and increases 39.8 times more than the rated mode without phase loss.

When the motor is under-loaded with a load-carrying factor of 75%, if a single-phase voltage loss occurs, the copper loss in the motor will be reduced by more than 2.7% compared to the total copper loss in phase loss at the rated load K=100% and increases 37.3 times more than that in the rated mode without phase loss. Losses in the motor produce heat that heats the motor, reducing efficiency, lifetime, and causing motor damage. Thus, when a single-phase voltage loss occurs, there must be a suitable motor protection method according to the load mode as well as the quality of the power supply to the motor.

Figure 9 shows speed ripple and torque ripple. Speed ripple is defined as the difference in the percentage between the maximum and minimum speeds relative to the mean speed. Torque ripple is defined as the difference in the percentage between the maximum and the minimum torques compared to the average torque.

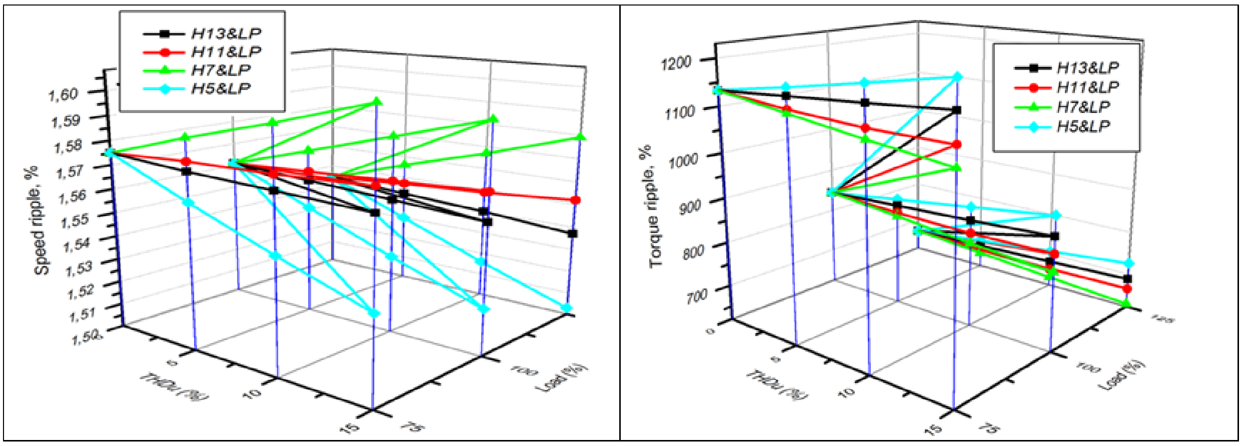

Fig. 9. Mechanical characteristics: Speed ripple and torque ripple.

Speed ripple decreases when a 5th order inverse harmonic is present and increases significantly when there is a 7th order harmonic in the case of a single-phase voltage loss. Speed ripple decreases with the increase of the load-carrying factor of the motor. As the 5th order harmonic increases, while the torque ripple increases leading to an increase in the vibration, the 7th order harmonic reduces the torque ripple in the case of single-phase voltage loss.

In the case when the power supply contains harmonics with the load factor K={75%, 100%, 125%}, the speed and torque ripples in the motor reach the highest of 0.0749% and 161.87% respectively.The torque ripple in the case of single-phase voltage loss with rated load (K= 100%) is 1.26 times higher than the under-load case (K=75%) and 0.75 times lower than in the overload case (K=125%). In addition, the torque ripple in this case is 23 times higher than in the normal working case

The speed ripple in the case of single-phase voltage loss with rated load (K= 100%) is 1.01 times higher than in the overload case (K=125%) and 0.99 times lower than in the under-load case (K=75%). In addition, the speed ripple in this case is 113 times higher than in the normal working case.

4. Conclusions

The paper has presented the influence of the single-phase voltage loss and the load-carrying mode on the working mode of the mine drainage pump motor in the nonsinusoidal power supply case. The results showed that when the single-phase voltage loss occurs, the speed and torque of the asynchronous motor decrease and fluctuate strongly, the copper losses on the stator and the rotor increase strongly, leading to an increase in the total loss in motor even in the case of underload, full load or overload.

In the case of nonsinusoidal power supply with single-phase voltage loss, copper losses in the rotor and stator circuits increase with increased voltage THD and load-carrying factor. The 5th order reverse harmonic increases copper loss in asynchronous motor the most. Higher harmonic components have less effect on copper loss in the motor.

The speed ripple decreases with the increase of the motor load factor. Additionally, it decreases in the presence of the 5^{th} order negative sequence harmonic but increases significantly in the presence of the 7^{th} order positive sequence harmonic. If the 5^{th} order negative sequence harmonic increases then the torque ripple increases. In contrast, the 7^{th} order positive sequence harmonic reduces the torque ripple in the case of single-phase voltage loss.

From the above analyses, the study of single-phase voltage loss in the case of nonsinusoidal power supply in the mine pump motor with different load-carrying modes is essential to determine the loss, working efficiency, thereby recommending users to have a suitable operating solution to improve the life of the mine drainage pump motor.

5. Acknowledgements

Paper was presented during the 6^{th} VIET-POL International Conference Scientific-Research Cooperation between Vietnam and Poland, 10-14.11.2021, HUMG, Hanoi, Vietnam.

6. References

1. Ovchinnikov, N.P., 2020. Recommendations for improving the operation efficiency of electric pumping units of mine drainage installations. In IOP Conference Series: Earth and Environmental Science. 548(5): 20-48.
2. Shang, D., 2017. Application research on testing efficiency of main drainage pump in coal mine using thermodynamic theories. International Journal of Rotating Machinery.
3. Papa, F., Radulj, D., Karney, B., Robertson, M., 2014. Pump energy efficiency field testing and benchmarking in Canada. Journal of Water Supply: Research and Technology-AQUA, 63(7): 570-577.
4. Kersting, W.H., 2005. Causes and effects of single-phasing induction motors. IEEE Transactions on Industry Applications, 41(6).
5. AQ 1012-2005 The Main Drainage System Safety Testing Inspection Specifications in Coal Mine. 2005. China Standards Press, Beijing, China.
6. Samir, M., Singh, G., Ahmed, N., Ahmed, H., 2013. Dynamic Performance Analysis of Three Phase Induction Motor with Single Phasing. In Proceedings of the Conference on Advances in Communication and Control Systems, Atlantis Press.
7. Donolo, P., Bossio, G., De Angelo, C., Garcia, G., Donolo, M., 2016. Voltage unbalance and harmonic distortion effects on induction motor power, torque and vibrations. Electric power systems research.
8. Bhattarai, P.D., 2013. Study on effects of supply voltage asymmetry and distortion on induction machine. A thesis, the Louisiana state University and Agricultural and Mechanical College. Faculty of the Louisianan State University and Agricultural and Mechanical College.
9. Lee, C.Y., 1999. Effects of unbalanced voltage on the operation performance of a three-phase induction motor. IEEE Transactions on Energy Conversion, 14(2): 202-208.

10. Mirabbasi, D., Seifossadat, G., Heidari, M., 2009. Effect of unbalanced voltage on operation of induction motors and itsdetection. In 2009 International Conference on Electrical and Electronics Engineering-ELECO. 1-189, IEEE.
11. Kersting, W.H., Phillips, W.H., 1997. Phase frame analysis of the effects of voltage unbalance on induction machines. IEEE Transactions on Industry Applications, 33(2): 415-420.
12. Gnacinski, P., 2008. Effect of unbalanced voltage on windingstemperature, operational life and loadcarryingcapacity of induction machine. Energy Conversion and Management, 49(4): 761-770.
13. Wang, Y.J., 2001. Analysis of effects of three-phase voltage unbalance on induction motors with emphasis on the angle of the complex voltage unbalance factor. IEEE Transactions on energy conversion, 16(3): 270-275.
14. Dekhandji, F.Z., Refoufi, L., Bentarzi, H., 2017. Quantitative assessment of three phase supply voltage unbalanceeffects on induction motors. International Journal of System Assurance Engineering and Management, 8(1): 393-406.
15. Quispe, E., Gonzalez, G., Aguado, J., 2004. Influence of unbalanced and waveform voltage on the performance characteristics of three-phase induction motors. In: Proceedings of international conference on renewable energy and power quality applications. Barcelona: Espana.
16. Gnaciński, P., Peplinsski, M., Hallmann, D., Jankowski, P., 2019. Induction cage machine thermal transientsunderlowered voltage quality. IET Electric Power Applications, 13(4): 479-486.
17. NEMA. Standard publications No. MG1. Motors and generators. Washington: published by national electrical manufactures association; 1993. Part 21 and part 30, 1-2.
18. Ngo, X.C., Do, N.Y., Tran, Q.H., 2020. The Influence of Voltage Quality on Asynchronous Motor Performance of EKG Excavator in Open Pit Mines–Vinacomin. Inżynieria Mineralna, 16(1): 139-145.
19. Nguyen, N. X. and Le, T. X, 2017. Evaluating effect of the voltage resonant caused by harmonics of nonlinear loads to capacitor banks located on Nam Mau Coal Company's 6kV electric grid (in Vietnamese), Journal of Mining and Earth Sciences, 58(2): 128-136, Available from: http://jmes.humg.edu.vn/en/archives?article=784.
20. Do, Y. N., Le, T. X., Nguyen, N. B. and Ngo, T. T., 2020. Impact of asymmetrical phenomena on asynchronous three-phase motors in operation mode, Journal of Mining and Earth Sciences, 61(3): 68-74, https://doi.org//10.46326/JMES.2020.61(3).08.
21. Sousa, S.V., Cabello, E.JJ., Sagastume, G.A., Cabello, U.MJ., 2019. Assessment of the energy efficiency estimation methods on induction motors considering real-time monitoring. Measurement, 136, 237-247.
22. Ding, X., Mi, C.C., 2011. Impact of inverter on losses and thermal characteristics of induction motors. International Journal of Power Electronics, 3(6), 641-651.
23. Al-Badri, M., Pillay, P., Angers, P., 2017. A novel in situ efficiency estimation algorithm for three-phase induction motors operating with distorted unbalanced voltages. IEEE Transactions on Industry Applications, 53(6), 5338-5347.
24. Yacamini, R., Chang, S.C., 1995. Noise and vibration from induction machines fedfromharmonic sources. IEEE Transactions on energy conversion, 10(2), 286-292.
25. El-Kharashi, E., Massoud, J.G., Al-Ahmar, M.A., 2019. The impact of the unbalance in both the voltage and the frequency on the performance of single and cascaded induction motors. Energy, 181: 561-575.
26. Amin, K.E., Hamouda, R.M., Abu-Siada, A., El Dessuki, M.A., 2016. Electromechanical oscillations of common-shaft cascaded induction motors driving a large mechanical load. Eighteenth International Middle East Power Systems Conference (MEPCON), pp. 645-650, IEEE.
27. Beleiu, H.G., Maier, V., Pavel, S.G., Birou, I., Pică, C.S., Dărab, P.C., 2020. Harmonics Consequences on Drive Systems with Induction Motor. Applied Sciences, 10(4): 1528.